Orbital fluctuation and phase transitions in iron-pnictides: a tight-binding Wannier function analysis

Z. P. Yin and W. E. Pickett

Department of Physics, University of California Davis, Davis, CA 95616

(Dated: November 29, 2009)

To perform a local orbital analysis of electronic and magnetic interactions, we construct the Wannier functions of the Fe $3d$ orbitals in the parent compounds of the newly discovered iron pnictide superconductors and use a tight binding representation to fit the first principles, density functional based Fe-derived bands. The calculated hopping parameters indicate that Fe $3d_{xz}$ have a larger amplitude to hop in the y than in the x direction (and analogously for $3d_{yz}$) electrons). Changes due to stripe antiferromagnetism, even if it is weak, enables the spin-majority electron in Fe $3d_{xz}$ (but not the $3d_{yz}$) orbital hop almost equally in both x and y directions. This change, counterintuitively, actually reinforces anisotropy, and may be relevant to the tetragonal-to-orthorhombic structural transition. This additional hopping channel alters the Fe $3d_{xz}$ bands near Fermi level, and its strength reflects the orbital magnetic moment and the total magnetic moment of Fe atom in the stripe antiferromagnetic phase. Insight is gained by comparing the band structures and Fe magnetic moments of LaFeAsO and LaFePO compounds. To take advantage of a kinetic energy gain from this additional hopping process, orbital fluctuation is favored, which reduces the ordered Fe magnetic moment in the stripe antiferromagnetic phase, consistent with experimental observations. We also affirm that the pnictide atom is influential in forming the stripe antiferromagnetism. Interlayer hopping of Fe $3d$ electrons in the z direction may inhibit fluctuations and thereby help to stabilize the ordered magnetic moment of Fe in the stripe antiferromagnetic phase.

I. BACKGROUND AND MOTIVATION

Since the first report from Hosono's group[1] of superconductivity at T_c=26 K in F-doped LaFeAsO, hundreds of experimental and theoretical papers on these iron-pnictide compounds have appeared, aimed at elucidating various properties, including synthesizing new compounds to achieve higher T_c, measuring basic quantities (e.g. magnetic susceptibility, NMR, ARPES), and modeling and simulating to obtain explanations and predictions. Thanks to these efforts, there are now several families of these iron pnictide superconductors, including the 1111-family (e.g. LaFeAsO, CaFeAsF), 122-family (e.g. $BaFe_2As_2$), 111-family (e.g. LiFeAs) and a more complicated 22426-family (e.g. $Fe_2As_2Sr_4Sc_2O_6$), with T_c up to 56 K.[2] Several aspects have been clarified: the superconductivity lies in primarily iron $3d$ bands[3] and is not phonon-mediated;[4] the ground state in most classes is a stripe antiferromagnetic phase with a significantly reduced Fe magnetic moment compared to theoretically calculated value;[5,6] it is a moderately correlated system where a Coulomb interaction U$\approx$3 eV might be appropriate.[7] There is discussion that the superconducting order parameter may have a new $s_\pm$ character.[8,9]

Despite a great deal of progress in understanding the electronic structure[10–12] and magnetic interactions,[13–15] some basic questions remain unresolved. One of them is: what causes the structural transition from tetragonal to orthorhombic in the parent compounds of iron-based superconductors? It is especially challenging in the 1111-compounds (e.g. LaFeAsO), where the structural transition is observed (when lowering the temperature) to occur before[16] the magnetic transition (from nonmagnetic to stripe antiferromagnetic, we denote it as Q_M AFM). It would have been natural to think that the stripe antiferromagnetic ordering of Fe provides the driving force for the structural transition because it introduces anisotropy. (See Table III in reference [17] for a summary of the structural transition temperature T_S and stripe antiferromagnetic transition temperature T_N of several iron pnictide compounds.)

Noting that the structural transition and magnetic transition occurs simultaneously in the 122-compounds (e.g. $BaFe_2As_2$), a possible argument is that the magnetism is in fact present, in the form of medium-range order, antiphase boundaries, etc., near the structural transition but its detection is greatly suppressed by strong spatial or temporal fluctuation. The suggestion by Mazin and Johannes that magnetic antiphase boundaries may be the dominant excitation[18] has already stimulated numerical estimations by the present authors.[19] With a time resolution of 10^{-15} s, photoemission experi-

ments by Bondino *et al.*[20] inferred a dynamic magnetic moment of Fe with magnitude of 1 μ_B in the nonmagnetic phase of $CeFeAsO_{0.89}F_{0.11}$, which is comparable to the ordered magnetic moment of Fe in the undoped antiferromagnetic CeFeAsO compound. The fluctuation strength should be much stronger in 1111-compounds than 122-compounds based on the fact that the measured Fe ordered magnetic moment in 1111-compounds ($\sim 0.4\ \mu_B$) is much less than in 122-compounds ($\sim 0.9\ \mu_B$) and they are much smaller than DFT predicted value ($\sim 2\ \mu_B$).[6,17] One factor is that interlayer coupling of FeAs layers is much stronger in 122-compounds than 1111-compounds because the interlayer distance in 122-compounds (~ 5.9-$6.5\ \mathring{A}$) is significantly smaller than 1111-compounds (~ 8.2-$9.0\ \mathring{A}$).[17] The interlayer interaction may help to stabilize the ordered Fe magnetic moment by reducing fluctuations.

In this paper we address the specific question of the strength, character, and spin-dependence of Fe-Fe coupling by using a Wannier function representation based on all five Fe $3d$ orbitals, and only these orbitals. Several previous studies of the electronic structure have noted the strong influence of the pnictide (or chalcogenide) orbitals and their positions.[6,21–24] While we do provide one example of the effect of the pnictogen atom (comparing LaFaAsO with LaFePO) in this paper, in most of our results we include the effect of the pnictogen precisely but indirectly through the Wannierization process and focus on an Fe-centric picture. With this local orbital representation we are able to provide additional insight into the competition between kinetic and on-site repulsion energetics in these materials.

II. CALCULATIONAL METHODS

We perform first principle calculations using the full-potential local-orbital code[25] (FPLO8) with local density approximation (LDA) exchange-correlation (XC) functional[26] (PW92) and the same experimental lattice constants and internal atomic coordinates for the compounds LaFeAsO, LaFePO, CaFeAsF, SrFeAsF, $BaFe_2As_2$, $SrFe_2As_2$, and $CaFe_2As_2$, as used in our previous work[6,11,19]. For the other two hypothetical compounds LaFeNO and LaFeSbO, the lattice constants and internal atomic coordinates are taken from the optimized equilibrium values of first principle calculations[27] done in the Q_M AFM phase using GGA (PBE) XC functional[28], since such calculations were proven
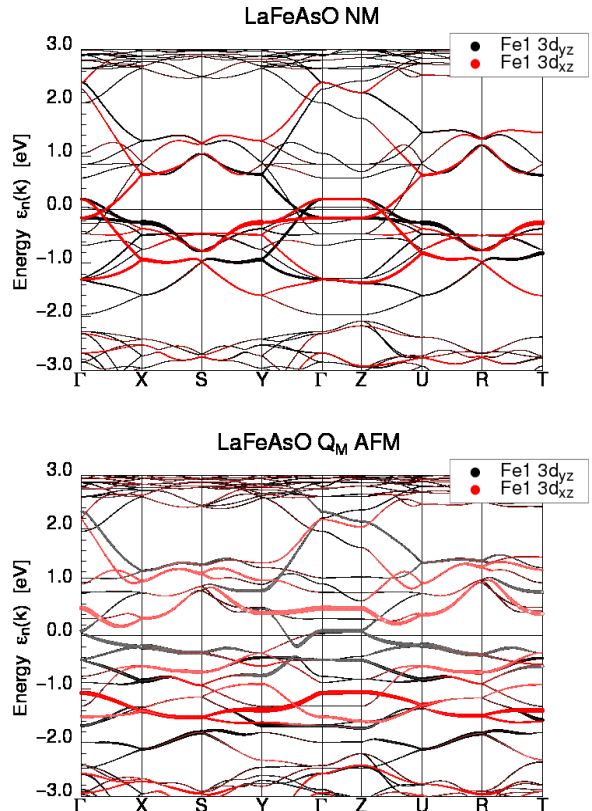

FIG. 1: LaFeAsO band structure with highlighted Fe $3d_{yz}$ and $3d_{xz}$ fatband characters in the NM (top panel) and Q_M AFM (bottom panel) phases. Compared to the NM phase, the Fe $3d_{xz}$ bands near Fermi level in the Q_M AFM phase, especially along $\Gamma-X$ and $\Gamma-Y$ directions, change dramatically due to the formation of the stripe antiferromagnetism with large ordered Fe magnetic moment of 1.9 μ_B.

to predict the correct equilibrium lattice constants and internal atomic coordinates compared to the experimental values in all the known iron pnictide compounds.[19,27]

To obtain the hopping parameters (which shall be discussed below), we have constructed real-space Wannier functions derived from Fe $3d$ orbitals in both NM and Q_M AFM phases in all the compounds mentioned above using the FPLO8 code. The Wannier functions used in this paper are constructed by projecting the Bloch functions from a specified energy range onto chosen atomic orbitals, following the method of Ku *et al.*[29,30] The resulting Wannier orbitals retain a symmetry that is common to both the atomic orbital and the point group symmetry of the site. These Wannier functions provide an explicit
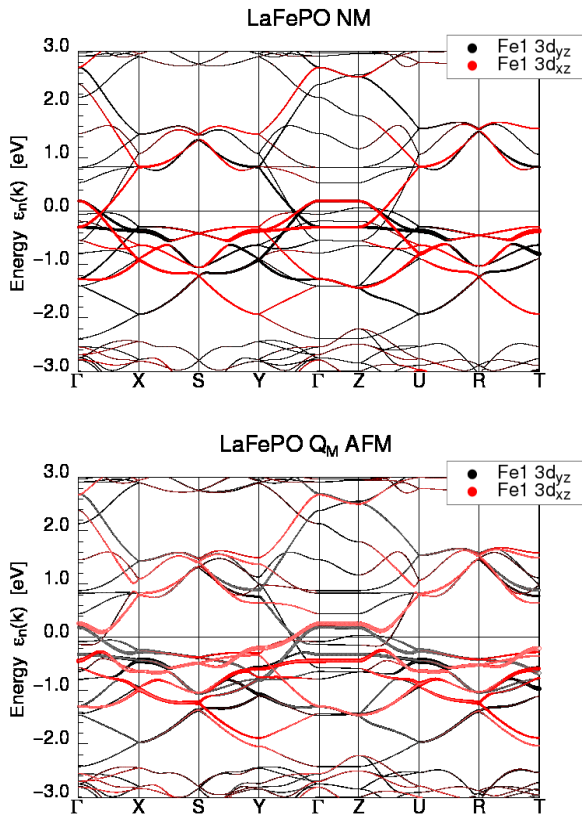
FIG. 2: LaFePO band structure with highlighted Fe $3d_{yz}$ and $3d_{xz}$ fatband characters in the NM (top panel) and Q_M AFM (bottom panel) phase. Compared to LaFeAsO, the Fe $3d_{xz}$ bands near Fermi level in the Q_M AFM phase change less significantly from the NM phase, due to the relatively small ordered Fe magnetic moment of 0.5 μ_B.

basis set of local orbitals that give a tight binding representation, complete with on-site energies and hopping amplitudes to neighbors as distant as necessary to represent the chosen bands. In this paper we project onto the conventional real Fe $3d$ orbitals, with the energy range corresponding to the region with strong Fe $3d$ character in the bands.

III. THE FE $3d_{yz}$ AND $3d_{xz}$ BANDS IN LAFEASO AND LAFEPO

Regarding the electronic structures (such as band structures, density of states, total energy, magnetic moment, etc.) in these compounds, a very important issue is the role of pnictide atom. Since the calculated Fe magnetic moment is much larger than its experimentally measured value in these parent com-

pounds, the electronic structure in the Q_M AFM phase cannot be taken too seriously. Some have tried to produce the experimental magnetic moment in their calculations, usually by applying a negative Coulomb interaction U parameter in LSDA+U method.[31,32] In this paper, we compare also a parallel system of LaFeAsO, namely LaFePO. The total energy of LaFePO in the Q_M AFM phase is slightly lower than the nonmagnetic phase by 2 meV/Fe.[11] The calculated Fe magnetic moment in the Q_M AFM phase is 0.52 μ_B, which is relatively close to the measured magnetic moment 0.36 μ_B in the Q_M AFM phase of LaFeAsO.[5,11] The band structures of LaFeAsO and LaFePO in the nonmagnetic and Q_M AFM phase are shown in Fig. 1 and 2, with highlighted Fe $3d_{yz}$ and $3d_{xz}$ characters. (We choose x direction along the stripe direction with aligned Fe spins, as shown in Fig. 3, then y direction is parallel to the anti-aligned Fe spins.) The nonmagnetic band structures of the two compounds are very similar, differing only in some fine details. However, the band structures in the Q_M AFM phase of the two compounds differ substantially, which can only be due to the difference in the Fe magnetic moment (1.9 vs. 0.5 μ_B).[6,11] The similarities and differences indirectly provide a way to study the effect of magnetic fluctuation on these compounds.

Figure 2 shows the influence of a weak stripe antiferromagnetism (0.5 μ_B) on the nonmagnetic band structure. The overall band structure remains the same except for some bands near the Fermi energy, where the main change is the separating of the Fe $3d_{xz}$ bands away from the Fermi level, which causes disappearance and change of topology of certain pieces of the Fermi surface of the Fe $3d_{xz}$ bands. Note that the Fe $3d_{yz}$ bands change insignificantly. This difference indicates that even a weak stripe antiferromagnetism has a very strong symmetry breaking effect on the $3d_{xz}$ and $3d_{yz}$ bands, which are equivalent in the nonmagnetic state. As a result, even a weak stripe antiferromagnetism induces a large anisotropy, let alone the much stronger (calculated) antiferromagnetism in FeAs-based compounds. (The much bigger anisotropy in the stripe AFM phase in LaFeAsO is evident by comparing Fig. 1 and 2.)
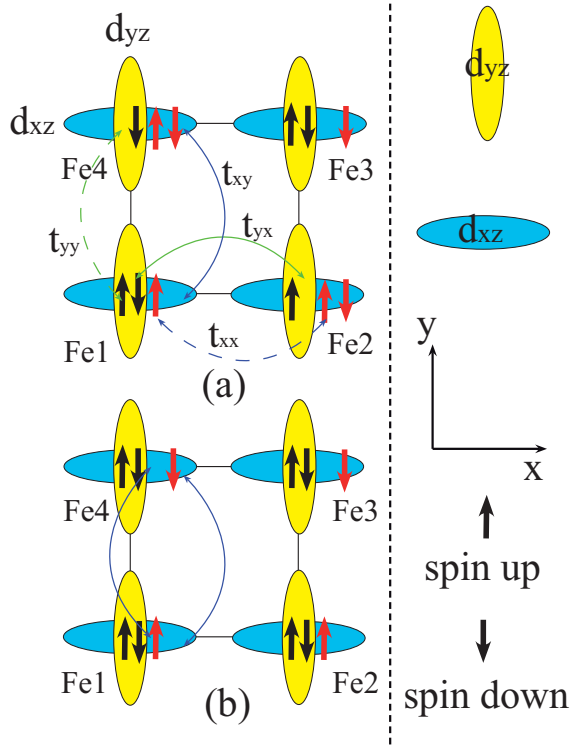
FIG. 3: (color online)Possible orbital orderings of iron in iron-pnictides. Left panel: Both (a) and (b) form the Q_M AFM ordering. However, (a) is favored because it gains more kinetic energy from nearest-neighbor hoppings according to second-order perturbation theory (see text). Right panel (from top to bottom) shows the simplified symbols for Fe $3d_{yz}$ and $3d_{xz}$ orbitals, the chosen x and y directions, up arrows for spin up electrons and down arrows for spin down electrons, where black arrows for $3d_{yz}$ orbital and red arrows for $3d_{xz}$ orbital.

IV. POSSIBLE MICROSCOPIC ORBITAL ORDERING OF THE FE $3d_{xz}$ AND $3d_{yz}$ ORBITALS

Due to the strong influence of stripe antiferromagnetism on the band structure, the orbital ordering of the Fe $3d_{xz}$ and $3d_{yz}$ electrons bears further consideration. Figure 3 shows two possible orbital orderings, both of which give rise to the Q_M AFM structure. t_{xy} denotes the hopping parameter of the $d_{xz} - d_{xz}$ hopping in the y direction, and t_{yx} the $d_{yz} - d_{yz}$ hopping in the x direction. In the non-

magnetic case,

$$t_{xy} = t_{yx} = t \tag{1}$$

and they differ by a small amount in the Q_M AFM state. t_{xx} denotes the $d_{xz} - d_{xz}$ hopping in the x direction, and t_{yy} the $d_{yz} - d_{yz}$ hopping in the y direction (see Fig. 3).

Let U and U' denote the intra-orbital and inter-orbital Coulomb repulsion, and J_H the inter-orbital Hund's exchange. According to second-order perturbation theory, the kinetic energy gain from the $d_{yz} - d_{yz}$ hopping in the x direction (Fig. 3a) is

$$\Delta E_{yx} = -t_{yx}^2/(U' - J_H). \tag{2}$$

A similar kinetic gain of

$$\Delta E_{xy} = -t_{xy}^2/(U' - J_H) \tag{3}$$

comes from the $d_{xz} - d_{xz}$ hopping in the y direction (Fig. 3a). t_{xx} and t_{yy} are much smaller and can be neglected (see Table I). Therefore, the total energy gain from NN hopping of Fig. 3a is

$$\Delta E(a) = \Delta E_{xy} + \Delta E_{yx} = -2t^2/(U' - J_H), \tag{4}$$

while it is

$$\Delta E(b) = -2t^2/U \tag{5}$$

for Fig. 3b. Because U is larger than $U' - J_H$, the orbital ordering in Fig. 3a is favored over Fig. 3b, by kinetic fluctuations. This result is in contrast to that of Lee *et al.*[33] who didn't consider the effect of t_{yx}.

V. TIGHT BINDING HOPPING PARAMETERS AND DISCUSSIONS

Figure 4 shows the Wannier functions of all five Fe $3d$ orbitals in both NM and Q_M AFM (majority spin) phases of LaFeAsO. The Wannier functions of all five Fe $3d$ orbitals of the minority spin in the Q_M AFM phase remain almost the same as in the NM phase, thus they are not shown. In the NM phase, all five Wannier functions for Fe $3d$ orbitals are well localized at the Fe site. In the Q_M AFM phase, the Wannier functions of the majority spin for $3d_{yz}$, $3d_{x^2-y^2}$ and $3d_{z^2}$ orbitals remain very similar to the corresponding Wannier functions in the NM phase, as shown in Fig. 4. However, the Wannier functions of the majority spin for $3d_{xz}$ and $3d_{xy}$ orbitals are

TABLE I: The hopping parameters (in eV) of the Fe1 $3d_{yz}$, $3d_{xz}$, and $3d_{xz}$ orbitals to all the five $3d$ orbitals of its nearest neighbor Fe2 and Fe4 atoms and next-nearest neighbor Fe3 atom in the nonmagnetic and Q_M AFM phases of LaFeAsO. The highlighted (italicized and boldface) entries are discussed in the text.

Fe1		yz			xz			xy	
	NM	Q_M		NM	Q_M		NM	Q_M	
		up	dn		up	dn		up	dn
Fe2 z^2	-0.12	-0.16	-0.08	0	0	0	0	0	0
x^2-y^2	0.34	0.42	0.28	0	0	0	0	0	0
yz	*-0.33*	*-0.42*	*-0.29*	0	0	0	0	0	0
xz	0	0	0	-0.06	**-0.29**	0.09	-0.22	-0.21	-0.20
xy	0	0	0	-0.22	-0.21	-0.20	**-0.18**	**-0.33**	**-0.07**
Fe4 z^2	0	0	0	-0.12	-0.11	-0.15	0	0	0
x^2-y^2	0	0	0	-0.34	-0.39	-0.34	0	0	0
yz	-0.06	-0.09	-0.09	0	0	0	-0.22	-0.21	-0.20
xz	0	0	0	*-0.33*	*-0.35*	*-0.35*	0	0	0
xy	-0.22	-0.20	-0.27	0	0	0	-0.18	-0.23	-0.23
Fe3 z^2	-0.10	-0.10	-0.11	-0.10	-0.12	-0.10	-0.17	-0.20	-0.21
x^2-y^2	0.10	0.09	-0.10	-0.10	-0.09	-0.09	0	0.02	-0.02
yz	*0.22*	*0.23*	*0.24*	0.08	0.12	0.08	-0.01	0.01	0
xz	0.08	0.08	0.12	*0.22*	*0.24*	*0.24*	-0.01	-0.02	0.03
xy	0.01	0	-0.01	0.01	-0.03	0.02	0.13	0.13	0.13

more delocalized in the Q_M AFM phase, with significant density at the nearest neighbor As sites, especially for the d_{xz} orbital. Therefore, the $3d_{xz}$ and $3d_{xy}$ orbitals of the majority spin mix more strongly with nearest-neighbor As $4p$ orbitals in the Q_M phase than in the NM phase.

Using these Wannier functions as the basis of the local orbitals in a tight binding representation, the hopping parameters are then obtained from matrix elements of the Wannier Hamiltonian from the FPLO8 code. The corresponding band structures of LaFeAsO and LaFePO are already shown in Fig. 1 and Fig. 2 and the resulting tight binding bands (not shown) fit very well the corresponding DFT-LSDA Fe-derived bands in both NM and stripe AFM phases. Table I shows the hopping parameters of the Fe1 $3d_{yz}$, $3d_{xz}$, and $3d_{xy}$ orbitals to all the $3d$ orbitals of its nearest neighbor Fe2 and Fe4 atoms and next nearest neighbor Fe3 atom in LaFeAsO compound. (See Fig. 3 for the definition of each Fe atom.)

The onsite energies (in eV) of all the five $3d$ orbitals in the NM phase and Q_M AFM phase in LaFeAsO and LaFePO are shown in Table II. In the Q_M AFM phase, the onsite energies are shown separately for both spin up (majority spin) and spin down (minority spin) orbitals. The hopping parameters reported here are very similar to the corresponding hopping parameters reported by Lee *et al.*[33] and Haule *et al.*[34], but are not directly comparable to those reported by Cao *et al.*[35] who mainly

considered the hoppings from As $4p$ orbitals to Fe $3d$ orbitals and to its nearest neighbor As $4p$ orbitals. As shown in Table I, in the NM phase, $t_{xy} = t_{yx} >> t_{xx} = t_{yy}$, which suggests that the hopping (through As atoms) of $d_{xz} - d_{xz}$ ($d_{yz} - d_{yz}$) in the y (x) direction of the electrons in Fe $3d_{xz}$ ($3d_{yz}$) orbital is favored over the x (y) direction. The hopping process for Fe $3d_{xz}$ ($3d_{yz}$) electrons is anisotropic. Global tetragonal symmetry is retained because the Fe $3d_{xz}$ and $3d_{yz}$ electrons hop in different directions, which enforces the equivalence of the x and y directions.

TABLE II: The onsite energies (in eV) of the d_{z^2}, $d_{x^2-y^2}$, d_{yz}, d_{xz}, and d_{xy} Fe orbitals in the NM and Q_M AFM phases in LaFeAsO and LaFePO. In the Q_M AFM phase, the onsite energies are shown separately for the spin up (majority spin) and spin down (minority spin) orbitals.

	LaFeAsO			LaFePO		
	NM	Q_M		NM	Q_M	
		up	dn		up	dn
z^2	-0.11	-0.95	0.18	-0.17	-0.35	-0.04
x^2-y^2	-0.27	-1.14	0.07	-0.27	-0.44	-0.14
yz	0.02	-0.67	0.23	-0.04	-0.19	0.07
xz	0.02	-0.70	0.21	-0.04	-0.21	0.07
xy	0.18	-0.50	0.40	0.23	0.13	0.30

In the Q_M AFM phase, the corresponding hopping parameters (both spin up and spin down) are either the same or very close to the NM value, ex-
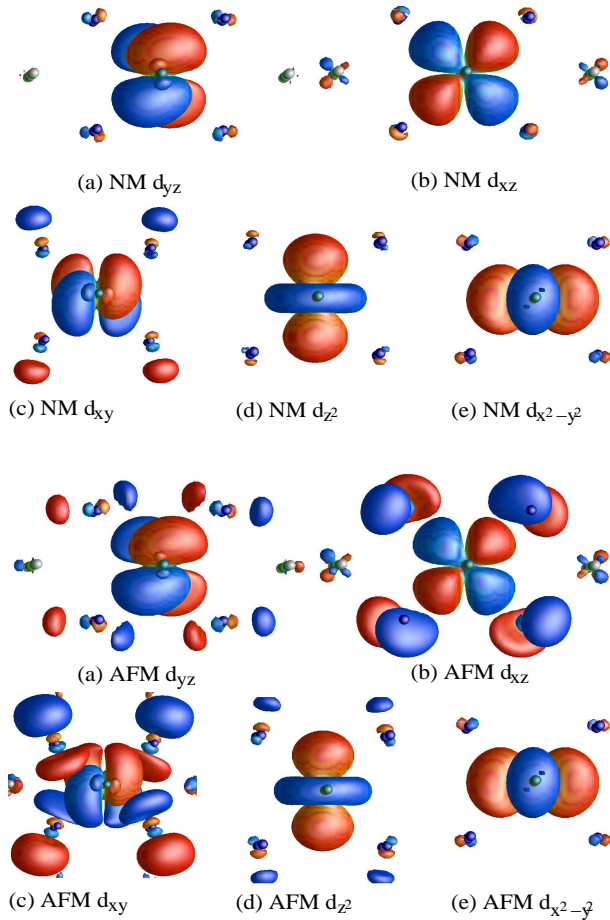
FIG. 4: LaFeAsO Wannier functions of Fe $3d$ orbitals in the NM (top panel) and Q_M AFM (bottom panel, for the majority spin) phases. (a) $3d_{yz}$, (b) $3d_{xz}$, (c) $3d_{xy}$, (d) $3d_{z^2}$, and (e) $3d_{x^2-y^2}$. The Wannier functions of Fe $3d$ orbitals for the minority spin in the Q_M AFM phase remain almost the same as in the NM phase. In the NM phase, these Wannier functions are well localized at the Fe site, however, in the Q_M AFM phase, the Wannier functions of the majority spin for the $3d_{xz}$ and $3d_{xy}$ orbitals are more delocalized, with significant density at the nearest-neighbor As sites. The isosurface is at the same value (density) in each panel.

cept for two cases. The first one is the $d_{xz} - d_{xz}$ hopping between parallel spin Fe neighbors (x direction) of a majority spin electron, whose absolute value increases significantly from the NM case (from -0.06 to -0.29, see the highlighted numbers in Table I). This opens an extra hopping channel in addition to the original $d_{xz} - d_{xz}$ hopping in the y direction. In the NM state, the electrons in the d_{xz} or d_{yz} or-

bitals can only hop in one direction (in the sense that the hopping parameters in other directions are relatively small). The dramatic change of the $3d_{xz}$ bands near Fermi level from NM to Q_M AFM can be traced to this difference.

The other case is the $d_{xy} - d_{xy}$ hopping also between parallel spin atoms (x direction). In the NM phase, the $d_{xy} - d_{xy}$ hoppings in both x and y directions are the same with an amplitude of 0.18 eV, which is consistent with its symmetry. In the Q_M AFM phase, this hopping in the y direction for both spins is slightly enhanced to 0.23 eV. However, the $d_{xy} - d_{xy}$ hopping in the x direction is significantly enhanced to 0.33 for the majority spin and suppressed to 0.07 for the minority spin. These differences shows that the symmetry that is broken by having both parallel spin (x direction) and antiparallel spin (y direction) neighbors introduces important broken symmetry in the d_{xy} orbital.

The magnitude of the changes of the hopping parameters in the two special cases mentioned above is directly related to the magnitude of the ordered Fe magnetic moment in the Q_M AFM state, which is evident by comparing the case of LaFeAsO and LaFePO (see Table I and III). The iron atom in the Q_M AFM state in the former compound has a large ordered magnetic moment of 1.9 μ_B while in the latter compound it is very weak, only 0.5 μ_B, in DFT-LSDA calculations. The difference in the ordered Fe magnetic moment is consistent with the change of hopping parameters of $d_{xz} - d_{xz}$ and $d_{xy} - d_{xy}$ in the x direction of the spin majority electron from the NM to the Q_M AFM state, as shown in Table I and Table III. In LaFeAsO, the former changes from -0.06 to -0.29 and the latter changes from -0.18 to -0.33, while in LaFePO, the former changes only from -0.09 to -0.15 and the latter changes only from -0.27 to -0.31.

The difference in the changes of the hopping parameters of each Fe $3d$ orbital from NM phase to Q_M AFM phase is related to the spin polarization of each orbital in the Q_M AFM phase, as shown in Table IV. The $3d_{xz}$ orbital has the largest moment (0.51 μ_B in LaFeAsO), followed by the $3d_{xy}$ orbital (0.48 μ_B in LaFeAsO). The other three orbitals have significantly smaller moments (less than 0.41 μ_B in LaFeAsO). It is clear that the orbital with larger orbital spin magnetic moment has bigger changes in the relevant hopping parameters. The difference of the relevant hopping parameters between LaFeAsO and LaFePO can also be traced to the difference in the orbital spin magnetic moment.

The transition to the Q_M AFM state is accompa-

TABLE III: The hopping parameters (in eV) of the Fe1 $3d_{yz}$, $3d_{xz}$, and $3d_{xz}$ orbitals to all the five $3d$ orbitals of its nearest neighbor Fe2 and Fe4 atoms and next-nearest neighbor Fe3 atom in the nonmagnetic and Q_M AFM phases of LaFePO.

Fe1		yz			xz			xy		
		NM	Q_M		NM	Q_M		NM	Q_M	
			up	dn		up	dn		up	dn
Fe2	z^2	-0.06	-0.07	-0.05	0	0	0	0	0	0
	x^2-y^2	0.42	0.44	0.41	0	0	0	0	0	0
	yz	*-0.37*	*-0.37*	*-0.34*	0	0	0	0	0	0
	xz	0	0	0	-0.09	**-0.15**	-0.03	-0.23	-0.23	-0.22
	xy	0	0	0	-0.23	-0.23	-0.23	**-0.27**	**-0.31**	**-0.24**
Fe4	z^2	0	0	0	-0.06	-0.06	-0.06	0	0	0
	x^2-y^2	0	0	0	-0.42	-0.43	-0.42	0	0	0
	yz	-0.09	-0.09	-0.09	0	0	0	-0.23	-0.24	-0.22
	xz	0	0	0	*-0.36*	*-0.36*	-0.36	0	0	0
	xy	-0.23	-0.22	-0.24	0	0	0	-0.27	-0.27	-0.28
Fe3	z^2	-0.09	-0.08	-0.08	-0.09	-0.09	-0.08	-0.24	-0.24	-0.24
	x^2-y^2	-0.13	0.13	-0.13	-0.13	-0.12	-0.13	0	0	0
	yz	*0.25*	*0.25*	*0.25*	0.09	0.10	0.09	0.04	0.04	0.05
	xz	0.09	0.08	0.10	*0.25*	*0.25*	*0.25*	0.04	0.04	0.05
	xy	-0.04	-0.05	-0.04	-0.04	-0.05	-0.04	0.16	0.16	0.16

TABLE IV: Occupation numbers and spin polarizations in $3d$ orbitals in the NM and Q_M AFM phases of LaFeAsO and LaFePO compounds. δn is the difference of the total occupation number in each orbital between the Q_M AFM phase and the NM phase. m is the spin magnetic moment in each orbital in the Q_M AFM phase.

	LaFeAsO					LaFePO				
	NM	Q_M				NM	Q_M			
		up	dn	δn	m		up	dn	δn	m
z^2	0.710	0.889	0.484	-0.05	0.405	0.688	0.747	0.639	0.010	0.108
x^2-y^2	0.573	0.798	0.454	0.104	0.344	0.542	0.593	0.502	0.011	0.091
yz	0.654	0.851	0.570	0.113	0.281	0.671	0.717	0.635	0.010	0.082
xz	0.654	0.855	0.349	-0.104	0.506	0.671	0.750	0.560	-0.032	0.190
xy	0.679	0.868	0.385	-0.105	0.483	0.666	0.711	0.618	-0.003	0.093

nied by an extra kinetic energy gain of

$$\Delta E_{xx} = -t_{xx}^2/(U' - J_H) \qquad (6)$$

from the hopping process of $d_{xz} - d_{xz}$ hopping in the x direction, which is comparable with ΔE_{xy}. (Note that ΔE_{xx} is negligible in the NM state.) A substantial extra kinetic energy gain can also be obtained from the $d_{xy} - d_{xy}$ hopping in the x direction. The anisotropy arises because the majority-spin electron in the $3d_{xz}$ orbital can hop in both directions (*i.e.* to both parallel and antiparallel spin neighbors), while others in the $3d_{xz}$ and $3d_{yz}$ orbitals can basically only hop in one direction. This anisotropy is reflected in a large symmetry lowering of the $3d_{xy}$ orbital in the AFM phase. The anisotropy leads to a large spin polarization (orbital spin magnetic moment) in the $3d_{xz}$ and $3d_{xy}$ orbital, which may also be related to the tetragonal to orthorhombic structural transition such that the lattice constant along the aligned-spin direction (x direction in this paper) becomes shorter than the other direction (y direction in this paper, thus $a < b$).

The additional $3d_{xz} - 3d_{xz}$ hopping and the enhancement of the $3d_{xy} - 3d_{xy}$ hoppings, both in the x direction of the spin majority electron, promote kinetic energy gain. However, as pictured in Fig. 3a, the $3d_{xz}$ spin up electron of Fe1 atom cannot hop in the x direction due to the Pauli principle. In order to take advantage of this extra kinetic energy gain of ΔE_{xx}, the spin up occupation number of the $3d_{xz}$ orbital should not be unity but instead must fluctuate. The same situation happens to the $3d_{xy}$ orbital. The competition between the kinetic energy gain and Pauli principle results in a reduced magnetic moment and is possibly one mechanism of orbital fluctuation.

TABLE V: The ratios of hopping parameters t_{xy}, t_{yx}, t_{xx} and t_{yy} in the NM and Q_M AFM phases of a few iron-pnictides.

compound (mag. mom.)		yz			xz		
		NM	Q_M up	dn	NM	Q_M up	dn
LaFeNO (1.86 μ_B)	t_{yx}/t_{xy}	-0.30	-0.33	-0.27	-0.30	-0.31	-0.31
	t_{yy}/t_{xx}	-0.03	-0.05	-0.05	-0.03	-0.14	0.06
LaFePO (0.52 μ_B)	t_{yx}/t_{xy}	-0.37	-0.37	-0.34	-0.36	-0.36	-0.36
	t_{yy}/t_{xx}	-0.09	-0.09	-0.09	-0.09	-0.15	-0.03
LaFeAsO (1.90 μ_B)	t_{yx}/t_{xy}	-0.33	-0.42	-0.29	-0.33	-0.35	-0.35
	t_{yy}/t_{xx}	-0.06	-0.09	-0.09	-0.06	-0.29	0.09
LaFeSbO (2.45 μ_B)	t_{yx}/t_{xy}	-0.26	-0.39	-0.21	-0.26	-0.28	-0.27
	t_{yy}/t_{xx}	-0.07	-0.11	-0.11	-0.07	-0.38	0.16
CaFeAsF (1.75 μ_B)	t_{yx}/t_{xy}	-0.36	-0.43	-0.34	-0.36	-0.37	-0.37
	t_{yy}/t_{xx}	-0.06	-0.08	-0.08	-0.06	-0.27	0.08
SrFeAsF (1.96 μ_B)	t_{yx}/t_{xy}	-0.35	-0.43	-0.31	-0.35	-0.37	-0.37
	t_{yy}/t_{xx}	-0.08	-0.10	-0.10	-0.08	-0.31	0.08
BaFe$_2$As$_2$ (1.88 μ_B)	t_{yx}/t_{xy}	-0.32	-0.40	-0.29	-0.32	-0.34	-0.34
	t_{yy}/t_{xx}	-0.08	-0.10	-0.10	-0.08	-0.28	0.07
SrFe$_2$As$_2$ (1.78 μ_B)	t_{yx}/t_{xy}	-0.33	-0.40	-0.31	-0.33	-0.34	-0.35
	t_{yy}/t_{xx}	-0.08	-0.10	-0.10	-0.08	-0.28	0.06
CaFe$_2$As$_2$ (1.67 μ_B)	t_{yx}/t_{xy}	-0.33	-0.38	-0.32	-0.33	-0.35	-0.35
	t_{yy}/t_{xx}	-0.08	-0.10	-0.10	-0.08	-0.28	0.06

A. Further Observations

Similar hopping parameters compared to LaFeAsO have been obtained for the CaFeAsF, SrFeAsF, and MFe$_2$As$_2$ (M=Ba, Sr, Ca) compounds, (which have similar FeAs layers), as shown in Table V. However, replacing As in LaFeAsO with other pnictides (N, P and Sb) results in similar t_{xy}, t_{yx} and t_{yy} but different t_{xx}. Compared to LaFeAsO, the t_{xx} for the majority spin electron in the Q_M AFM phase is reduced for LaFeNO and LaFePO, but enhanced in LaFeSbO. The importance of the pnictide for the formation of the Q_M AFM phase is evident.

Another important factor is the interlayer hoppings. The interlayer distance of FeAs layers in 1111-compounds is in the range of 8.2 -9.0 $\overset{\circ}{A}$ and it is much smaller in 122-compounds, ranging from 5.9 $\overset{\circ}{A}$ to 6.5 $\overset{\circ}{A}$. The interlayer hopping parameters of Fe $3d$ electrons in the z direction are negligible in 1111-compounds but become substantial for certain hoppings in 122-compounds, especially in CaFe$_2$As$_2$, whose interlayer distance of FeAs layers is only 5.9 $\overset{\circ}{A}$. Certain interlayer hopping parameters are as large as 0.15 eV for $3d_{xy}$ and $3d_{z^2}$ orbitals, and 0.07 eV for $3d_{yz}$, $3d_{xz}$ and $3d_{x^2-y^2}$ orbitals, calculated in the Q_M AFM phase for CaFe$_2$As$_2$, which has the small-

est interlayer distance.

The large interlayer hopping parameters for the Fe $3d_{xy}$ orbital, which at first sight seems very surprising, becomes clear by noting that the $3d_{xy}$ Wannier orbital is strongly distorted from its symmetric atomic shape to its nearest neighbor As atoms above and below the Fe plane, as shown in Fig. 4. This extension in the z direction will favor interlayer hoppings, especially when the interlayer distance is small, as in the case of CaFe$_2$As$_2$. For comparison, the interlayer hopping parameters (if not zero) are less than 0.01 eV in LaFeAsO. The increasing hopping of Fe $3d$ electrons in the z direction increases the interlayer coupling, and may inhibit fluctuations and thereby help to stabilize the ordered Fe magnetic moment in the Q_M AFM phase. The k_z dispersion correlates with the experimental observations that the measured Fe magnetic moments in the Q_M AFM phase are significantly larger in 122-compounds ($\sim$ 0.9 μ_B) than 1111-compounds ($\sim$ 0.4 μ_B).

VI. SUMMARY

In this paper, we have compared the band structures of LaFeAsO and LaFePO, in both NM and Q_M AFM phases, and find that the stripe antiferromagnetism affects very differently the various Fe $3d$ orbital characters, even when the stripe antiferromagnetism is weak. By comparing the hopping parameters of several 1111-compounds and 122-compounds, we find that the pnictide atom and the structure are influential in the formation of Q_M AFM phase. This information was obtained from a tight-binding representation for Fe $3d$ electrons based on first principles Wannier functions.

In the nonmagnetic phase the electrons in Fe $3d_{xz}$ and $3d_{yz}$ orbitals have very different amplitudes to hop in the x and y directions, connected to the positions of pnictide atoms. Anti-intuitively, this "anisotropy" is almost gone for majority spin electrons in the AFM phase, when the $3d_{xz}$ (or $3d_{yz}$) electron can hop equally to parallel and antiparallel neighbors (both x and y directions). This additional hopping may have some importance for the structural transition to orthorhombic symmetry. This anisotropy is accompanied by a lowering of symmetry in the $3d_{xy}$ Wannier function as well. The (large) changes in the near neighbor hopping parameters of the $3d_{xz}$ and $3d_{xy}$ orbitals in the x direction is important in leading to the much larger orbital spin magnetic moments of these two orbitals than the other three orbitals. The significant enhancement

of the hopping parameters of the $3d_{xz} - 3d_{xz}$ and $3d_{xy} - 3d_{xy}$ hoppings of the majority spin electrons to parallel spin neighbors affects energetics that influence the magnetic and structural transitions.

The anisotropy in hopping in the Fe $3d_{yz}$, $3d_{xz}$, and $3d_{xy}$ orbitals also favors orbital fluctuation by providing extra kinetic processes, which are partly compensated by the Pauli principle which inhibits the hopping processes, and which we expect to enhance fluctuations in the corresponding orbital occupation numbers (orbital fluctuation). Such fluctuations would reduce the ordered Fe magnetic moment in the Q_M phase, bringing them closer to the observed ordered moments. Interlayer hoppings of the Fe $3d$ electrons in the z direction may also help to stabilize the Fe magnetic moment in the Q_M AFM phase.

[1] Y. Kamihara, T. Watanabe, M. Hirano, and H. Hosono, J. Amer. Chem. Soc. **130**, 3296 (2008).

[2] C. Wang, L. J. Li, S. Chi, Z. W. Zhu, Z. Ren, Y. K. Li, Y. T. Wang, X. Lin, Y. K. Luo, S. Jiang, X. F. Xu, G. H. Cao, and Z. A. Xu, Europhysics Letters **83**, 67006 (2008).

[3] R. H. Liu, T. Wu, G. Wu, H. Chen, X. F. Wang, Y. L. Xie, J. J. Yin, Y. J. Yan, Q. J. Li, B. C. Shi, W. S. Chu, Z. Y. Wu, and X. H. Chen Nature **459**, 64 (2009).

[4] L. Boeri, O. V. Dolgov, and A. A. Golubov Phys. Rev. Lett. **101**, 026403 (2008).

[5] C. de la Cruz, Q. Huang, J. W. Lynn, J. Li, W. Ratcliff, J. L. Zaretsky, H. A. Mook, C. F. Chen, J. L. Luo, N. L. Wang, and P. Dai, Nature **453**, 899 (2008).

[6] Z. P. Yin, S. Lebègue, M. J. Han, B. P. Neal, S. Y. Savrasov, and W. E. Pickett, Phys. Rev. Lett. **101**, 047001 (2008).

[7] M. Aichhorn, L. Pourovskii, V. Vildosola, M. Ferrero, O. Parcollet, T. Miyake, A. Georges, and S. Biermann, Phys. Rev. B **80**, 085101 (2009).

[8] I. I. Mazin, D. J. Singh, M. D. Johannes, and M. H. Du, Phys. Rev. Lett. **101**, 057003 (2008).

[9] Y. Nagai, N. Hayashi, N. Nakai, H. Nakamura, M. Okumura, and M. Machida, New J. Phys. **10**, 103026 (2008).

[10] D. J. Singh and M.-H. Du, Phys. Rev. Lett. **100**, 237003 (2008).

[11] S. Lebègue, Z. P. Yin, and W. E. Pickett, New J. Phys. **11**, 025004 (2009).

[12] I. I. Mazin, M. D. Johannes, L. Boeri, K. Koepernik, and D. J.Singh, Phys. Rev. B **78**, 085104 (2008).

[13] A. N. Yaresko, G.-Q. Liu, V. N. Antonov, and O. K. Andersen, Phys. Rev. B **79**, 144421 (2009).

[14] M. J. Han, Q. Yin, W. E. Pickett, and S. Y. Savrasov, Phys. Rev. Lett. **102**, 107003 (2009).

[15] M. D. Johannes and I. I. Mazin, Phys. Rev. B **79**, 220510 (2009).

[16] M.A. McGuire, A. D. Christianson, A. S. Sefat, B. C. Sales, M. D. Lumsden, R. Jin, E. A. Payzant, D. Mandrus, Y. Luan, V. Keppens, V. Varadarajan, J. W. Brill, R. P. Hermann, M. T. Sougrati, F. Grandjean, and G. J. Long, Phys. Rev. B **78**, 054529 (2008).

[17] K. Ishida, Y. Nakai, H. Hosono, J. Phys. Soc. Jpn. **78**, 062001 (2009).

[18] I. I. Mazin and M. D. Johannes, Nature Physics **5**, 141 (2009).

[19] Z. P. Yin and W. E. Pickett, Phys. Rev. B **80**, 144522 (2009).

[20] F. Bondino, E. Magnano, M. Malvestuto, F. Parmigiani, M. A. McGuire, A. S. Sefat, B. C. Sales, R. Jin, D. Mandrus, E. W. Plummer, D. J. Singh, and N. Mannella, Phys. Rev. Lett. **101**, 267001 (2008).

[21] V. Vildosola, L. Pourovskii, R. Arita, S. Biermann, and A. Georges, Phys. Rev. B **78**, 064518 (2008).

[22] L. D. Belashchenko and V. P. Antropov, Phys. Rev. B **78**, 212505 (2008).

[23] T. Yildirim, Phys. Rev. Lett. **102**, 037003 (2009).

[24] M. Berciu, I. Elfimov, and G. A. Sawatzky, Phys. Rev. B **79**, 214507 (2009).

[25] K. Koepernik and H. Eschrig Phys. Rev. B **59**, 1743 (1999).

[26] J. P. Perdew and Y. Wang, Phys. Rev. B **45**, 13244 (1992).

[27] Z. P. Yin, *Microscopic Mechanisms of Magnetism and Superconductivity Studied from First Principle Calculations*, Ph.D dissertation (2009).

[28] J. P. Perdew, K. Burke, and M. Ernzerhof, Phys. Rev. Lett. **77**, 3865 (1996).

[29] W. Ku, H. Rosner, W. E. Pickett, and R. T. Scalettar, Phys. Rev. Lett. **89**, 167204 (2002).

[30] W. Ku, H. Rosner, W. E. Pickett, and R. T. Scalettar J. Solid State Chem. **171**, 329 (2003).

[31] J. Dai, Z. Y. Li, J. L. Yang, J. G. Hou, arXiv:0808.0065 (2008).

[32] M. D. Johannes, private communication (2009).

[33] C.-C. Lee, W.-G. Yin, and W. Ku, arXiv:0905.2957 (2009).

[34] K. Haule and G. Kotliar, New J. Phys. **11**, 025021 (2009).

[35] C. Cao, P. J. Hirschfeld, and H.-P. Cheng, Phys. Rev. B **77**, 220506(R) (2008).